

HAAR WAVELETS-BASED APPROACH FOR QUANTIFYING CREDIT PORTFOLIO LOSSES

JOSEP J. MASDEMONT, LUIS ORTIZ-GRACIA

ABSTRACT. This paper proposes a new methodology to compute *Value at Risk* (VaR) for quantifying losses in credit portfolios. We approximate the cumulative distribution of the loss function by a finite combination of Haar wavelet basis functions and calculate the coefficients of the approximation by inverting its Laplace transform. The Wavelet Approximation (WA) method is specially suitable for non-smooth distributions, often arising in small or concentrated portfolios, when the hypothesis of the Basel II formulas are violated. To test the methodology we consider the Vasicek one-factor portfolio credit loss model as our model framework. WA is an accurate, robust and fast method, allowing to estimate VaR much more quickly than with a Monte Carlo (MC) method at the same level of accuracy and reliability.

1. INTRODUCTION

It is very important for banks to manage risks originated from their business activities. In particular, the credit risk underlying the credit portfolio is often the largest risk in a bank. The measure of credit risk is used to assign capital in order to absorb potential losses arising from the credit portfolio.

The Vasicek model is the basis of the Basel II IRB approach. It is a Gaussian one factor model such that default events are driven by a latent common factor that is assumed to follow a Gaussian distribution, also called the *Asymptotic Single Risk Factor* (ASRF) model. Under this model, loss only occurs when an obligor defaults in a fixed time horizon. If we assume certain homogeneity conditions, this one factor model leads to a simple analytic asymptotic approximation for the loss distribution and *Value at Risk* (VaR). This approximation works well for a large number of small exposures but can underestimate risks in the presence of exposure concentrations (see [Gie06]).

Concentration risks in credit portfolios arise from an unequal distribution of loans to single borrowers (*name concentration*) or different industry or regional sectors (*sector* or *country concentration*). Moreover, certain dependencies like, for example, direct business links between different borrowers, can increase the credit risk in a portfolio since the default of one borrower can cause the default of a dependent second borrower. This effect is called *default contagion* and is linked to both name and sector concentration.

In credit risk management one is particularly interested in the portfolio loss distribution. Since the portfolio loss is usually modeled as a sum of random variables, the main task is to evaluate the probability density function (PDF) of such a sum. The PDF of a sum of random variables is equal to the convolution of the respective PDFs of the individual asset loss distributions. The analytical evaluation of this convolution is a difficult problem and even, computationally, is very intensive. In full generality is impractical for realistic size portfolios.

Monte Carlo simulation is a standard method for measuring the risk of a credit portfolio. However this method is very time-consuming when the size of the portfolio increases. Computations can become unworkable in many situations, taking also into account the issue that financial companies have to re-balance their credit portfolios frequently.

For all these reasons, several methods have been developed during the last years. The saddle point approximation due to [Mar01] gives an analytical approximation of the Laplace inversion of the moment generating function (MGF). This method has been improved by [Mar06] based on conditional independence models. [Gla07] applies the methodology developed by [Aba00] to the single-factor Merton model. First, the Bromwich integral is approximated by an infinite series using the trapezoidal rule and second, the convergence of the infinite series is accelerated by a method called Euler summation. They have shown that the cumulative distribution function (CDF) is comparatively accurate in the regions associated with small losses but it worsens in the tail region, i.e. for big losses. This is due to the fact that the infinite series obtained by the Euler summation is an alternating series where each term is very big in absolute value.

Another approach to numerically invert the Laplace transform has been studied by [Hoo82] and [Ahn03]. Following [Aba00], it consists in applying the Poisson algorithm to approximate the Bromwich integral by an infinite series, and then to use the quotient-difference (QD) algorithm to accelerate its slow convergence. We refer to this approach as *the Hoog algorithm*. Also [Tak08] applies this methodology to the multi-factor Merton model. The numerical examples presented in these papers show that, in contrast with the Euler summation technique, Hoog algorithm is quite efficient in measuring tail probabilities.

Our contribution is a novel methodology for computing VaR via numerically inverting the Laplace transform of the CDF of the loss function, once we have approximated it by a finite sum of Haar wavelets basis functions. Up to certain extent, the idea is similar to the one in [Aba96], which uses Laguerre polynomials instead of wavelets. In the financial context, [Hav09] also performs a Laplace transform inversion for option pricing purposes using a series expansion in terms of the Franklin hat wavelets. The authors numerically compute the coefficients of the approximation by minimizing the average of squared errors between the true option prices and estimated prices. The technique to get the coefficients in our method is quite different in the sense that, our analytical treatment provides an expression for the wavelet coefficients by means of the Cauchy's integral theorem.

Then one can compute them using an ordinary trapezoidal rule avoiding this way the infinite series of [Gla07] and [Tak08]. The power of the WA method mostly resides in the good balance between computational time and accuracy both for small and high loss levels, and also for a wide range of portfolios, independent of concentration types and sizes. The saddle point approach, as an asymptotic method, tends in general to work better for high VaR confidence levels when the size of the portfolio increases. Moreover, if the loss distribution is not smooth due to exposure concentration, a straightforward implementation may be insufficient. Finally, it is important to remark that Haar wavelets are naturally capable to reproduce the step-like form distribution derived from the Vasicek model, even when dealing with extremely small or concentrated portfolios, as will be shown in the section of numerical examples.

The remaining parts of the paper are organized as follows. In the following section we present the one-factor Gaussian copula model and we define VaR as the risk measure used to quantify losses in the Basel II Accord. In section three we present the basic theory underlying the Haar wavelet basis system used for the approximation detailed in section four. Finally, using several numerical examples, we show the speed, robustness and accuracy of the WA method in section five, while section six is devoted to conclusions.

2. PORTFOLIO LOSS AND VALUE AT RISK

To represent the uncertainty about future events, we specify a probability space $(\Omega, \mathcal{F}, \mathbb{P})$ with sample space Ω , σ -algebra \mathcal{F} , probability measure \mathbb{P} and with filtration $(\mathcal{F}_t)_{t \geq 0}$ satisfying the usual conditions. We fix a time horizon $T > 0$. Usually T equals one year.

Consider a credit portfolio consisting of N obligors. Any obligor n can be characterized by three parameters: the *exposure at default* E_n , the *loss given default* which without loss of generality we assume to be 100% and the *probability of default* P_n , assuming that each of them can be estimated from empirical default data. The exposure at default of an obligor denotes the portion of the exposure of the obligor that is lost in case of default. Let D_n be the default indicator of obligor n taking the following values

$$D_n = \begin{cases} 1, & \text{if obligor } n \text{ is in default,} \\ 0, & \text{if obligor } n \text{ is not in default,} \end{cases}$$

Let L be the portfolio loss given by:

$$L = \sum_{n=1}^N L_n,$$

where $L_n = E_n \cdot D_n$.

To test our methodology we consider the Vasicek one-factor Gaussian copula model as our model framework. The Vasicek model is a one period default model,

i.e., loss only occurs when an obligor defaults in a fixed time horizon. Based on Merton's firm-value model, to describe the obligor's default and its correlation structure, we assign to each obligor a random variable called firm-value. The firm-value of obligor n at time T , $V_n(T)$, is represented by a common, standard normally distributed factor Y component (the state of the world or business cycle, usually called systematic factor) and an idiosyncratic noise component ϵ_n :

$$V_n(T) = \sqrt{\rho_n}Y + \sqrt{1 - \rho_n}\epsilon_n,$$

where Y and $\epsilon_n, \forall n \leq N$ are i.i.d. standard normally distributed.

In case that $\rho_n = \rho$ for all n , the parameter ρ is called the common asset correlation. The important point is that conditional to the realization of the systematic factor Y , the firm's values and defaults are independent. From now on, we assume ρ_n to be constant.

Let us explain in detail the meaning of systematic and idiosyncratic risk. The first one can be viewed as the macro-economic conditions and affect the credit-worthiness of all obligors simultaneously. The second one represents conditions inherent to each obligor and this is why they are assumed to be independent of each other.

In the Merton model, obligor n defaults when its firm-value falls below the threshold level T_n , defined by $T_n \equiv \Phi^{-1}(P_n)$, where $\Phi^{-1}(x)$ denotes the inverse of the standard normal cumulative distribution function. The probability of default of obligor n conditional to a realization $Y = y$ is then given by,

$$p_n(y) \equiv \mathbb{P}(V_n < T_n \mid Y = y) = \Phi\left(\frac{T_n - \sqrt{\rho}y}{\sqrt{1 - \rho}}\right).$$

Consequently, the conditional probability of default depends on the systematic factor, reflecting the fact that the business cycle affects the possibility of an obligor's default.

Let us consider a portfolio with N obligors and let F be the cumulative distribution function of L . Without loss of generality, we can assume $\sum_{n=1}^N E_n = 1$ and consider

$$F(x) = \begin{cases} \bar{F}(x), & \text{if } 0 \leq x \leq 1, \\ 1, & \text{if } x > 1, \end{cases}$$

for a certain \bar{F} defined in $[0, 1]$.

Let $\alpha \in (0, 1)$ be a given confidence level (usually α of interest are very close to 1). The α -quantile of the loss distribution of L in this context is called *Value at Risk* (VaR):

$$l_\alpha = \inf\{l \in \mathbb{R} : \mathbb{P}(L \leq l) \geq \alpha\} = \inf\{l \in \mathbb{R} : F(l) \geq \alpha\}.$$

This is the measure chosen in the Basel II Accord for the computation of capital requirement, meaning that a bank that manages its risks according to Basel II, must reserve capital by an amount of l_α to cover potential extreme losses.

3. THE HAAR BASIS WAVELETS SYSTEM

Consider the space $L^2(\mathbb{R}) = \{f : \int_{-\infty}^{+\infty} |f(x)|^2 dx < \infty\}$. For simplicity we can view this set as the set of functions $f(x)$ which get small in magnitude fast enough as x goes to plus and minus infinity.

A general structure for wavelets in $L^2(\mathbb{R})$ is called a *Multi-resolution Analysis* (MRA). We start with a family of closed nested subspaces,

$$\cdots \subset V_{-2} \subset V_{-1} \subset V_0 \subset V_1 \subset V_2 \subset \cdots$$

in $L^2(\mathbb{R})$ where,

$$\bigcap_{j \in \mathbb{Z}} V_j = \{0\}, \quad \overline{\bigcup_{j \in \mathbb{Z}} V_j} = L^2(\mathbb{R}),$$

and

$$f(x) \in V_j \iff f(2x) \in V_{j+1}.$$

If these conditions are met, then there exists a function $\phi \in V_0$ such that $\{\phi_{j,k}\}_{k \in \mathbb{Z}}$ is an orthonormal basis of V_j , where,

$$\phi_{j,k}(x) = 2^{j/2} \phi(2^j x - k).$$

In other words, the function ϕ , called the *father function*, generates an orthonormal basis for each V_j subspace.

Let us define W_j in such a way that $V_{j+1} = V_j \oplus W_j$. This is, W_j is the space of functions in V_{j+1} but not in V_j , and so, $L^2(\mathbb{R}) = \sum_j V_j \oplus W_j$. Then (see [Dau92]) there exists a function $\psi \in W_0$ such that defining,

$$\psi_{j,k}(x) = 2^{j/2} \psi(2^j x - k),$$

$\{\psi_{j,k}\}_{k \in \mathbb{Z}}$ is an orthonormal basis of W_j and $\{\psi_{j,k}\}_{j,k \in \mathbb{Z}}$ is a wavelet basis of $L^2(\mathbb{R})$. The ψ function is called *mother function* and the $\psi_{j,k}$ functions are known as *wavelet functions*.

For any $f \in L^2(\mathbb{R})$ a projection map of $L^2(\mathbb{R})$ onto V_m ,

$$\mathcal{P}_m : L^2(\mathbb{R}) \rightarrow V_m,$$

is defined by means of

$$(1) \quad \mathcal{P}_m f(x) = \sum_{j=-\infty}^{m-1} \sum_{k=-\infty}^{k=+\infty} d_{j,k} \psi_{j,k}(x) = \sum_{k \in \mathbb{Z}} c_{m,k} \phi_{m,k}(x),$$

where $d_{j,k} = \int_{-\infty}^{+\infty} f(x) \psi_{j,k}(x) dx$ are the wavelet coefficients and the $c_{m,k} = \int_{-\infty}^{+\infty} f(x) \phi_{m,k}(x) dx$ are the scaling coefficients. Note that the first part in (1) is a truncated wavelet series. If j were allowed to go to infinity, we would have the full wavelet summation. The second part of (1) gives an equivalent sum in terms of the scaling functions $\phi_{m,k}$. Considering higher m values (i.e. when more terms are used), the truncated series representation of the function f improves. There exists also an interesting relation between the wavelet coefficients and the scaling coefficients at different scales:

$$(2) \quad c_{j,k} = \frac{c_{j+1,2k} + c_{j+1,2k+1}}{\sqrt{2}}, \quad d_{j,k} = \frac{c_{j+1,2k} - c_{j+1,2k+1}}{\sqrt{2}}.$$

To develop our work we consider Haar wavelets (see [Dau92]). Using these wavelets, V_j is the set of $L^2(\mathbb{R})$ functions which are constant on each interval of the form $[\frac{k}{2^j}, \frac{k+1}{2^j})$ for all integers k . In this case the father and mother functions are given by,

$$\phi(x) = \begin{cases} 1, & \text{if } 0 \leq x < 1, \\ 0, & \text{otherwise,} \end{cases}$$

and

$$\psi(x) = \begin{cases} 1, & \text{if } 0 \leq x < \frac{1}{2}, \\ -1, & \text{if } \frac{1}{2} \leq x < 1, \\ 0, & \text{otherwise.} \end{cases}$$

As opposed to Fourier series, a key fact about using wavelets is that wavelets can be moved (choosing the k value), stretched or compressed (choosing the j value) to accurately represent the local properties of a function. Moreover, $\phi_{j,k}$ is nonzero only inside the interval $[\frac{k}{2^j}, \frac{k+1}{2^j})$. In what follows we take worth of this fact to compute VaR without the need of knowing the whole distribution of the loss function.

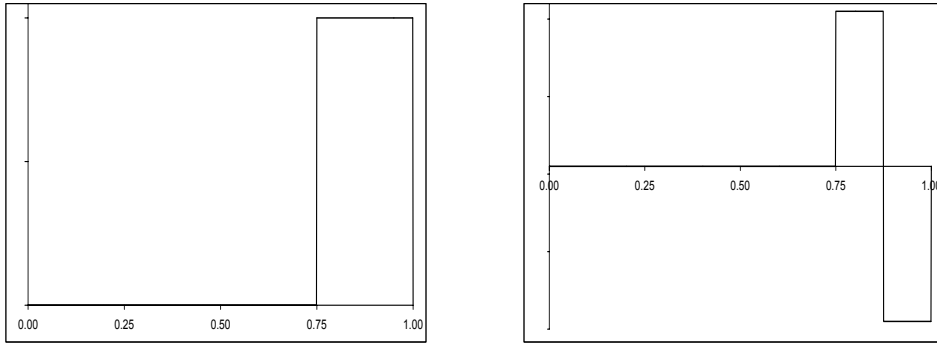


FIGURE 1. Scaling $(\phi_{2,3})$ and wavelet $(\psi_{2,3})$ functions.

4. HAAR WAVELETS APPROXIMATION

Let us note a property regarding the CDF \bar{F} previously defined. Since the loss can take only a (very big) finite number of discrete values (2^N at most), the PDF of the loss function is a sum of Dirac delta functions and then the CDF

is a discontinuous function. Moreover, the stepped form of the CDF makes Haar wavelets a natural and very well-suited approximation procedure.

4.1. Laplace Transform Inversion. Since $\bar{F} \in L^2([0, 1])$, according to the theory of MRA we can approximate \bar{F} in $[0, 1]$ by a summation of scaling functions,

$$(3) \quad \bar{F}(x) \approx \bar{F}_m(x), \quad \bar{F}_m(x) = \sum_{k=0}^{2^m-1} c_{m,k} \phi_{m,k}(x),$$

and

$$(4) \quad \bar{F}(x) = \lim_{m \rightarrow +\infty} \bar{F}_m(x).$$

We recall that in our one-factor model framework, if the systematic factor Y is fixed, default occurs independently since the only remaining uncertainty is the idiosyncratic risk. The MGF conditional to Y is thus given by the product of each obligor's MGF:

$$\begin{aligned} M_L(s; Y) &\equiv \mathbb{E}(e^{-sL} | Y) = \prod_{n=1}^N \mathbb{E}(e^{-sE_n D_n} | Y) \\ &= \prod_{n=1}^N [1 - p_n(y) + p_n(y)e^{-sE_n}]. \end{aligned}$$

Notice that we are assuming non stochastic LGD. Taking the expectation value of this conditional MGF yields the unconditional MGF,

$$\begin{aligned} (5) \quad M_L(s) &\equiv \mathbb{E}(e^{-sL}) = \mathbb{E}(\mathbb{E}(e^{-sL} | Y)) \\ &= \mathbb{E}(M_L(s; Y)) = \mathbb{E} \left[\prod_{n=1}^N [1 - p_n(y) + p_n(y)e^{-sE_n}] \right] \\ &= \int_{\mathbb{R}} \prod_{n=1}^N [1 - p_n(y) + p_n(y)e^{-sE_n}] \frac{1}{\sqrt{2\pi}} e^{-\frac{y^2}{2}} dy. \end{aligned}$$

But if f is the probability density function of the loss function, then the unconditional MGF is also the Laplace transform of f :

$$(6) \quad M_L(s) \equiv \mathbb{E}(e^{-sL}) = \int_0^{+\infty} e^{-sx} f(x) dx = \tilde{f}(s).$$

Also, as we have noticed before,

$$(7) \quad f(x) = \sum_{i=1}^{2^N} \mu_i \delta(x - x_i), \quad x_1, x_2, \dots, x_{2^N} \in [0, 1].$$

where $\delta(x - x_i)$ is the Dirac delta at x_i . Each Dirac delta can be thought as a density distribution of a unit of mass concentrated in the point x_i (i.e.

$\int_0^{+\infty} g(x)\delta(x-x_i)dx = g(x_i)$, for every test function $g(x)$). Probabilistically, a distribution like (7) corresponds to a situation where only the scenarios x_1, x_2, \dots, x_{2^N} are feasible and with respective probabilities $\mu_1, \mu_2, \dots, \mu_{2^N}$. Of course these probabilities must be positive and sum up to 1. This is,

$$\sum_{i=1}^{2^N} \mu_i = 1.$$

As it is also well known in the context of generalized functions, the derivative of the Heaviside step function is a Dirac delta. In this context (and of course in the context of regular functions) we can integrate by parts the expression (6) and use the approximation (3) to conclude that,

$$\begin{aligned} M_L(s) &= \int_0^{+\infty} e^{-sx} F'(x) dx = e^{-s} + s \int_0^1 e^{-sx} \bar{F}(x) dx \\ (8) \quad &\approx e^{-s} + s \int_0^1 \left[e^{-sx} \sum_{k=0}^{2^m-1} c_{m,k} \phi_{m,k}(x) \right] dx \\ &= e^{-s} + 2^{\frac{m}{2}} s \sum_{k=0}^{2^m-1} c_{m,k} \tilde{\phi}_{m,k}(s), \end{aligned}$$

where,

$$\tilde{\phi}_{m,k}(s) = \frac{1}{s} e^{-s \frac{k}{2^m}} (1 - e^{-s \frac{1}{2^m}})$$

is the Laplace transform of the basis function $\phi_{m,k}(x)$.

Observing that $\tilde{\phi}_{m,k}(s) = \tilde{\phi}_{m,0}(s) e^{-s \frac{k}{2^m}}$ and making the change of variable $z = e^{-s \frac{1}{2^m}}$, the expression (8) is cast into,

$$Q(z) \equiv \sum_{k=0}^{2^m-1} c_{m,k} z^k \approx \frac{M_L(-2^m \ln(z)) - z^{2^m}}{2^{\frac{m}{2}} (1-z)}.$$

Here we note that although $Q(z)$ is not defined at $z = 0$, the limit

$$\lim_{z \rightarrow 0} Q(z) = c_{m,0} = \frac{\int_{\mathbb{R}} \prod_{n=1}^N [1 - p_n(y)] \frac{1}{\sqrt{2\pi}} e^{-\frac{y^2}{2}} dy}{2^{\frac{m}{2}}}$$

exists and so,

$$\bar{Q}(z) \equiv \begin{cases} Q(z) & \text{if } z \neq 0 \\ \lim_{z \rightarrow 0} Q(z) & \text{if } z = 0 \end{cases}$$

is analytic inside the disc of the complex plane $\{z : |z| < r\}$ for $r < 1$, since the singularity in $z = 0$ is avoidable. Then, given the generating function $\bar{Q}(z)$, we

can obtain expressions for the coefficients $c_{m,k}$ by means of the Cauchy's integral formula. This is,

$$c_{m,k} = \frac{1}{2\pi i} \int_{\gamma} \frac{Q(z)}{z^{k+1}} dz, \quad k = 1, \dots, 2^m - 1 \quad (z \neq 0)$$

where γ denotes a circle of radius r , $0 < r < 1$, about the origin.

Considering now the change of variable $z = re^{iu}$, $0 < r < 1$ we have,

$$\begin{aligned} c_{m,k} &= \frac{1}{2\pi r^k} \int_0^{2\pi} \frac{Q(re^{iu})}{e^{iku}} du \\ (9) \quad &= \frac{1}{2\pi r^k} \int_0^{2\pi} [\Re(Q(re^{iu})) \cos(ku) + \Im(Q(re^{iu})) \sin(ku)] du \\ &= \frac{2}{\pi r^k} \int_0^{\pi} \Re(Q(re^{iu})) \cos(ku) du, \end{aligned}$$

and by means of the ordinary trapezoidal rule, we can evaluate this integral with the required accuracy to obtain the coefficients.

As a matter of fact, in the numerical examples section we see that when computing VaR values at 99.9% confidence level, taking 2^m subintervals we converge towards the Monte Carlo result. Also is worth to mention that the MGF in the expression (5) is also accurately computed using a Gauss-Hermite quadrature formula with 20 nodes.

4.2. VaR computation. It can be easily proved that

$$0 \leq c_{m,k} \leq 2^{-\frac{m}{2}}, \quad k = 0, 1, \dots, 2^m - 1,$$

and

$$0 \leq c_{m,0} \leq c_{m,1} \leq \dots \leq c_{m,2^m-1}.$$

Considering an approximation in a level of resolution m , VaR can now be quickly computed with m coefficients due to the compact support of the basis functions. Observe that due to the approximation (3) we have,

$$\bar{F}(l_{\alpha}) \approx 2^{\frac{m}{2}} \cdot c_{m,\bar{k}}$$

for a certain $\bar{k} \in \{0, 1, \dots, 2^m - 1\}$. Thus, we can simply start searching l_{α} by means of the following simple iterative procedure: first we compute $\bar{F}_m(\frac{2^m-1}{2^m})$. If $\bar{F}_m(\frac{2^m-1}{2^m}) > \alpha$ then we compute $\bar{F}_m(\frac{2^m-1-2^{m-2}}{2^m})$, otherwise we compute $\bar{F}_m(\frac{2^m-1+2^{m-2}}{2^m})$, and so on. This algorithm finishes after m steps storing the \bar{k} value such that $\bar{F}_m(\frac{\bar{k}}{2^m})$ is the closest value to α in our m resolution approximation.

In fact, due to the stepped shape of the Haar wavelets approximation, $\bar{F}_m(\xi) = \bar{F}_m(\frac{\bar{k}}{2^m})$, for all $\xi \in [\frac{\bar{k}}{2^m}, \frac{\bar{k}+1}{2^m})$. In what follows let us take, $l_{\alpha,m}^W = \frac{2\bar{k}+1}{2^{m+1}}$, the

middle point of this interval, as the VaR value computed by means of this wavelet algorithm at scale m .

Let us also consider the relative error at scale m defined by,

$$\text{RE}(\alpha, m) = \frac{|l_{\alpha, m}^W - l_{\alpha}|}{l_{\alpha}}.$$

Assuming that l_{α} is well approximated by a value, l_{α}^M , obtained by means of a Monte Carlo method that will be taken as benchmark, as is common in this kind of studies, we will use the estimation,

$$\text{RE}(\alpha, m) \simeq \frac{|l_{\alpha, m}^W - l_{\alpha}^M|}{l_{\alpha}^M}.$$

5. NUMERICAL EXAMPLES

In this section we present a comparative study to calculate VaR using the Wavelet Approximation and the Monte Carlo method. As it is well known, MC has a strong dependence between the size of the portfolio and the computational time. When the size increases, MC becomes a very big time consuming method.

Real situations in financial companies show the existence of strong concentrations in their credit portfolios, while Basel II formulae to calculate VaR are supported under unrealistic hypothesis, such as infinite number of obligors with small exposures. For these reasons, we also test our methodology with small and concentrated portfolios.

Portfolio	N	P_n	E_n	ρ	HHI	$\frac{1}{N}$
P1	100	0.21%	$\frac{C}{n}$	0.15	0.0608	0.0100
P2	1000	1.00%	$\frac{C}{n}$	0.15	0.0293	0.0010
P3	1000	0.30%	$\frac{C}{n}$	0.15	0.0293	0.0010
P4	10000	1.00%	$\frac{C}{n}$	0.15	0.0172	0.0001
P5	20	1.00%	$\frac{1}{N}$	0.5	0.0500	0.0500
P6	10	0.21%	$\frac{C}{n}$	0.5	0.1806	0.1000

TABLE 1. Portfolios selected for the numerical examples. In each case, C is a constant such that $\sum_{n=1}^N E_n = 1$.

We consider six portfolios ranging from 10 to 10000 obligors as described in Table 1. In order to consider concentrated portfolios, we have taken $E_n = \frac{C}{n}$ (where C is a constant such that $\sum_{n=1}^N E_n = 1$), except for portfolio P5 which is totally diversified. We provide also the Herfindahl-Hirschman index (HHI)

for quantifying exposure concentration. This index can take values from $\frac{1}{N}$ to 1 (this latter value corresponds to a portfolio with only 1 obligor). Well-diversified portfolios with a very large number of very small exposures have a HHI value close to $\frac{1}{N}$, whereas heavily concentrated portfolios can have a considerably higher HHI value. We note that P5 is a small and completely diversified portfolio while P6 is a small but strongly concentrated one. The correlation parameter ρ , which measures the degree of the obligor's exposure to the systematic risk factor, and the probabilities of default P_n have been taken as representative examples but in real scenarios have to be estimated from empirical data since higher correlations may lead to higher losses in the credit portfolio. Similarly, the potential loss increases when considering higher probabilities of default. This fact will be shown when comparing the VaR value of portfolios P2 and P3 where the remaining parameters are unchanged.

The main numerical results are displayed in Table 2. We have computed¹ the VaR value at 99.9% confidence level with the WA method at scales 8, 9 and 10 and also the VaR value using the MC method with 5×10^6 random scenarios, which serve us as a benchmark. For WA we take 20 nodes of Gauss-Hermite quadrature to evaluate the MGF and 2^m subintervals for the trapezoidal rule to compute the coefficients in (9). Plots at scales 9 and 10 corresponding to portfolios P1, P2, P3 and P4 can be seen in figures 2, 3, 4 and 5 respectively.

Portfolio	$l_{0.999,8}^W$	$l_{0.999,9}^W$	$l_{0.999,10}^W$	$l_{0.999}^M$
P1	0.1934 (0.04%)	0.1963 (1.56%)	0.1938 (0.29%)	0.1933
P2	0.1934 (1.02%)	0.1924 (0.50%)	0.1929 (0.75%)	0.1914
P3	0.1426 (1.46%)	0.1416 (0.77%)	0.1411 (0.42%)	0.1405
P4	0.1616 (0.06%)	0.1611 (0.37%)	0.1616 (0.06%)	0.1617

TABLE 2. Results of 99.9% VaR computation with Wavelet Approximation at scales 8, 9 and 10 and Monte Carlo simulations with 5×10^6 random scenarios. RE estimations are shown in parenthesis.

We provide as well the computational time in seconds in Table 3 both for MC method and WA method at scales 8, 9 and 10. WA at scale 10 give us very accurate results in a short computational time when compared with Monte Carlo. RE estimations for portfolios P1 and P4 at scale 8 are less than 0.1%, displaying already very accurate and fast computed approximations (specially for P4 which is a big portfolio), while portfolios P2, P3 and P4 are very well approximated

¹Computations have been carried out sequentially in a GNU-Linux laptop with Intel CPU Core 2 T7500, 2.2GHz, 2GB RAM and using the gcc compiler with optimization level 2.

at scale 9, with computational time needs reducing to 3.3, 3.2 and 32 seconds respectively.

In order to assess the robustness of the WA method we increased up to 100 the number of nodes in the Gauss-Hermite quadrature. With this setting we computed VaR values at 99.9%, 99.99% and 99.999% confidence levels at scale 10 for portfolios P1, P2, P3 and P4. The results obtained in all cases were coincident with the errors with respect to MC using only 20 nodes.

Portfolio	$l_{0.999,8}^W$	$l_{0.999,9}^W$	$l_{0.999,10}^W$	$l_{0.999}^M$
P1	0.2	0.3	0.7	65.9
P2	1.6	3.3	6.5	549.0
P3	1.6	3.2	6.5	546.9
P4	16.1	32.0	64.2	1053.9

TABLE 3. Computation time (in seconds) for portfolios P1, P2, P3 and P4 to compute the VaR value at 99.9% confidence level.

We have also assessed the robustness of the WA method doubling the number of subintervals used in the trapezoidal rule of integration, to compute the wavelet coefficients at scale 10 for portfolios P1, P2, P3 and P4. Numerical results are presented in Table 4. The VaR value at 99.9% confidence level is omitted since we get the same value using 2^m or 2^{m+1} subintervals. However we can observe differences at higher confidence levels. While RE estimations for VaR values at 99.99% computed with 2^m subintervals remain small, VaR values at 99.999% demand clearly more subintervals than 2^m . Increasing the number of subintervals up to 2^{m+1} , estimated RE reduce drastically for the 99.999% confidence level, showing that, when we go very deep in the tail, more subintervals in the trapezoidal rule have to be taken.

We have shown the suitability of the WA method to deal with concentration in portfolios of considerable size like P1, P2, P3 and P4. It is remarkable how the Haar wavelets are naturally capable of detecting jumps in the cumulative distribution function, making the approximation very precise at both small and high loss levels. To demonstrate that this interesting property still remains in small portfolios, we consider P5 and P6 plotted in figure 6, both at scale 10. Since P5 and P6 are very small portfolios, the non-smooth features appear accentuated. However the MC and WA plots are indistinguishable one from the other, showing again the fast convergence of the WA method towards MC for the Vasicek model.

Portfolio	2^{10}		2^{11}		MC	
	$l_{0.9999,10}^W$	$l_{0.99999,10}^W$	$l_{0.9999,10}^W$	$l_{0.99999,10}^W$	$l_{0.9999}^M$	$l_{0.99999}^M$
P1	0.2271 (0.79%)	0.3130 (4.84%)	0.2271 (0.79%)	0.2993 (0.26%)	0.2253	0.2985
P2	0.2642 (0.28%)	0.3696 (9.16%)	0.2642 (0.28%)	0.3462 (2.24%)	0.2634	0.3386
P3	0.1821 (0.43%)	0.2563 (9.84%)	0.1821 (0.43%)	0.2388 (2.30%)	0.1813	0.2334
P4	0.2280 (0.60%)	0.3306 (11.18%)	0.2271 (0.17%)	0.3071 (3.30%)	0.2267	0.2973

TABLE 4. VaR values at 99.99% and 99.999% confidence levels for portfolios P1, P2, P3 and P4 using 2^m and 2^{m+1} subintervals (case $m = 10$) for the trapezoidal rule. MC with 5×10^6 random scenarios and RE (shown inside brackets) are also provided.

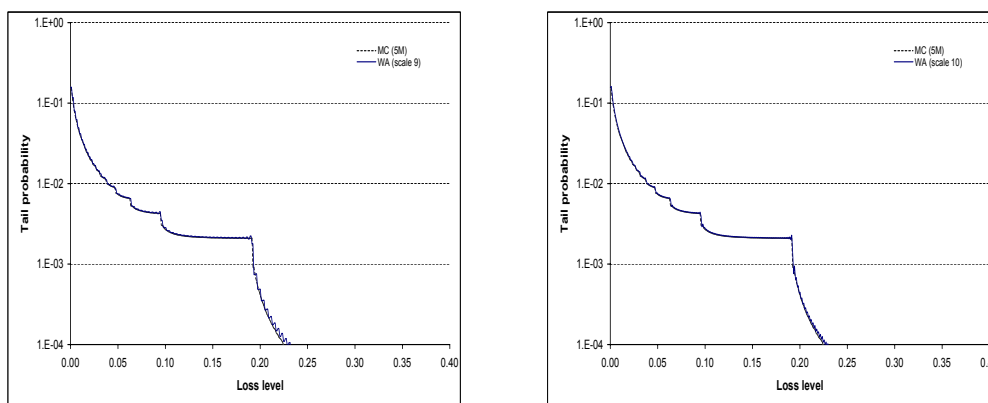


FIGURE 2. Tail probability approximation of portfolio P1 with $m = 9$ and $m = 10$.

6. CONCLUSIONS

We have presented a numerical approximation to the loss function based on Haar wavelets. First of all we approximate the discontinuous distribution of the loss function by a finite summation of Haar scaling functions, and then we calculate the coefficients of the approximation by inverting its Laplace transform. Due to the compact support property of the Haar system, only a few coefficients are needed for the VaR computation.

We have shown the performance of the numerical approximation in six sample portfolios. These results, among other simulations, show that the method is applicable and very accurate to different sized portfolios needing also of short

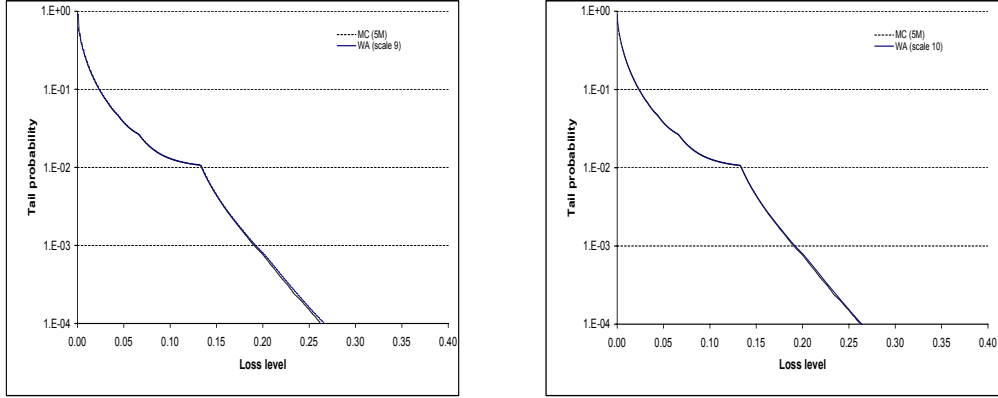


FIGURE 3. Tail probability approximation of portfolio P2 with $m = 9$ and $m = 10$.

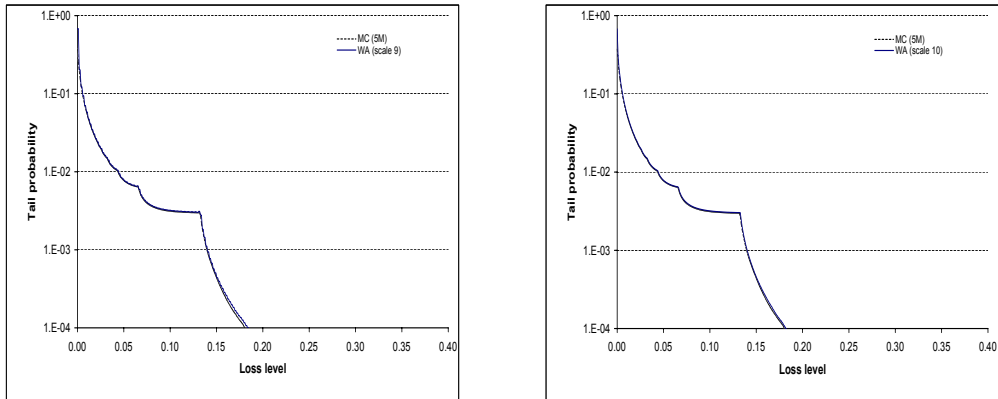


FIGURE 4. Tail probability approximation of portfolio P3 with $m = 9$ and $m = 10$.

time computations. Moreover, the Wavelet Approximation is robust since the method is very stable under changes in the parameters of the model. The stepped form of the approximated distribution makes the Haar wavelets natural and very suitable for the approximation.

We also remark that the algorithm is valid for continuous cumulative distribution functions, and that it can be used in other financial models without making

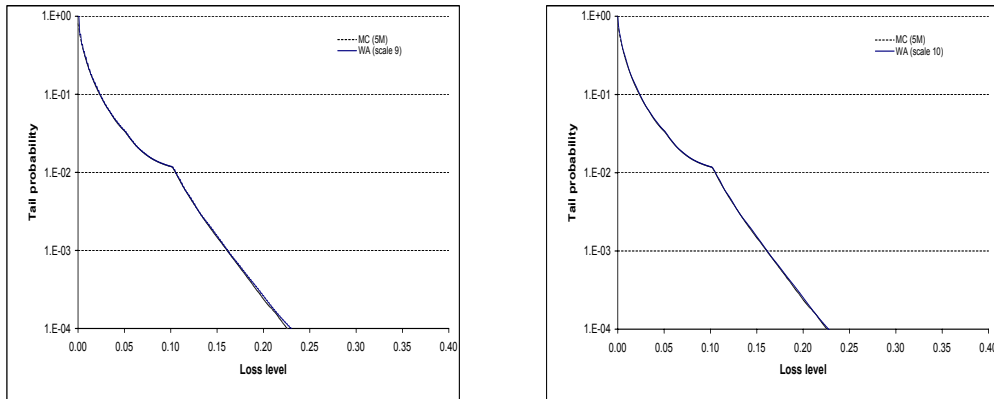


FIGURE 5. Tail probability approximation of portfolio P4 with $m = 9$ and $m = 10$.

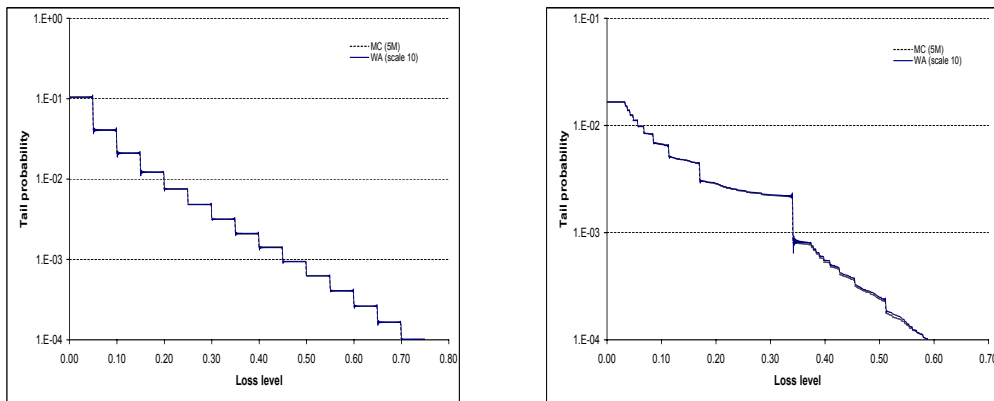


FIGURE 6. Tail probability approximation of portfolio P5 (left) and P6 (right) at scale $m = 10$.

conceptual changes in the development. For instance, we can easily introduce stochastic loss given default (just changing a bit the unconditional moment generating function) and to consider the multi-factor Merton model as the model framework as well.

ACKNOWLEDGEMENTS

This work has been partially supported by MICINN-FEDER grant MTM2009-06973 and CUR-DIUE grant 2009SGR859. The authors want to thank the reviewers for their comments and suggestions.

REFERENCES

- [Aba96] J. Abate, G.L. Choudhury and W. Whitt (2000). On the Laguerre method for numerically inverting Laplace transforms. *Journal on Computing*. Vol 8. No. 4.
- [Aba00] J. Abate, G.L. Choudhury and W. Whitt (2000). An introduction to numerical transform inversion and its application to probability models. *Computational Probability*, ed. W.K. Grassman, Kluwer, Norwell, MA. pp. 257-323.
- [Ahn03] J. Ahn, S. Kang and Y. Kwon (2003). A flexible inverse Laplace transform algorithm and its application. *Computing* 71. 115-131.
- [Dau92] I. Daubechies (1992). *Ten lectures on wavelets*. CBMS-NSF Regional Conference Series in Applied Mathematics. SIAM.
- [Gie06] G. Giese (2006). A saddle for complex credit portfolio models. *RISK* (July), 84-89.
- [Gla07] P. Glasserman and J. Ruiz-Mata (2007). Computing the credit loss distribution in the Gaussian copula model: a comparison of methods. *Journal of Credit Risk* 3. 33-66.
- [Hav09] E. Haven, X. Liu, C. Ma and L. Shen. Revealing the implied risk-neutral MGF from options: The wavelet method. *Journal of Economics Dynamics & Control* 33. 692-709.
- [Hoo82] F. de Hoog, J. Knight and A. Stokes (1982). An improved method for numerical inversion of Laplace transforms. *SIAM Journal on Scientific and Statistical Computing* 3. 357-366.
- [Mar01] R. Martin, K. Thompson and C. Browne (2001). Taking to the saddle. *RISK* (June), 91-94.
- [Mar06] R. Martin and R. Ordovás (2006). An indirect view from the saddle. *RISK* (October), 94-99.
- [Tak08] Y. Takano and J. Hashiba (2008). A novel methodology for credit portfolio analysis: numerical approximation approach. Available at www.defaultrisk.com.

JOSEP J. MASDEMONT

DEPARTAMENT DE MATEMÀTICA APLICADA I
 UNIVERSITAT POLITÈCNICA DE CATALUNYA
 DIAGONAL 647
 08028 BARCELONA, SPAIN
E-mail address: josep@barquins.upc.edu

LUIS ORTIZ-GRACIA

CENTRE DE RECECA MATEMÀTICA
 CAMPUS DE BELLATERRA EDIFICI C
 08193 BELLATERRA
 BARCELONA, SPAIN
E-mail address: lortiz@crm.cat